Source identification for fine aerosols in Mammoth Cave National Park

Weixiang Zhao, Philip K. Hopke *

Department of Chemical Engineering, and Center for Air Resources Engineering and Science, Clarkson University, P.O. Box 5708, Potsdam, NY 13699, USA

Abstract

In this study, positive matrix factorization (PMF) was applied to the chemical composition data of the ambient $PM_{2.5}$ collected at the Mammoth Cave National Park, an IMPROVE site in Kentucky. Eight individual carbon fractions, four organic carbons (OCs), pyrolyzed organic carbon (OP) and three elemental carbons (ECs), were provided to the analysis. Nine sources including the well-distinguished gasoline emission and diesel emission were identified. Also, the back trajectories indicated the crustal factor in this study were likely caused by Saharan dust storms in the summer. The apportionment of nine sources was: gasoline emission (6.7%), diesel emission (3.1%), summer secondary sulfate (49.0%), winter secondary sulfate (0.6%), OP-rich secondary sulfate (16.2%), secondary nitrate (2.8%), Intercontinental dust plus soil (4.9%), wood smoke (13.6%), and aged sea salt (3.2%). The results of this study will help regularize the pollution control strategies in rural areas of Kentucky and upper mid-western US while demonstrating the feasibility of applying carbon fractions to the source apportionment of rural upper-Midwestern areas.
© 2005 Elsevier B.V. All rights reserved.

Keywords: Positive matrix factorization; Source apportionment; Mammoth Cave National Park; OC/EC thermal fractions; Diesel emission; Gasoline emission

1. Introduction

A relationship between human mortality/morbidity and particulate matter (PM) concentrations has been observed (Dockery et al., 1993; Gauderman et al., 2000). Also, the evidence for a significant role of traffic-related emissions on public health has been reported (Cyrys et al.,

---

2003; de Hartog et al., 2003; Brauer et al., 2002; 2003; Hoek et al., 2002). Thus, the ability to effectively identify the possible particle sources including the diesel/gasoline emissions becomes increasingly important.

In this study, the aerosol chemical composition data collected at the Interagency Monitoring of Protected Visual Environments (IMPROVE) site at the Mammoth Cave National Park, Kentucky was analyzed. In addition to the element measurements, eight temperature resolved carbon fractions, four organic carbons (OC), pyrolyzed organic carbon (OP) and three elemental carbons (EC), were provided. In the previous analyses on ambient aerosols (Polissar et al., 2001; Song et al., 2001), PMF could not clearly resolve carbonaceous particle sources, especially various types of vehicle emissions, because of their similar profiles in terms of total OC and EC and similar emission patterns. Recent studies of the use of temperature-resolved carbon fractions in the PMF analysis of the PM data from Seattle, WA (Maykut et al., 2003), Atlanta, GA (Kim et al., 2004), Washington, DC (Kim and Hopke, 2004a), Brigantine, NJ (Kim and Hopke, 2004b), and San Gorgonio, CA (Zhao and Hopke, 2004), have suggested that diesel and spark-ignition emissions can be separated well. Therefore, the objectives of this study are to identify the aerosol sources in the Mammoth Cave National Park area and to demonstrate the feasibility of using carbon fractions to resolve the motor vehicle sources in the upper Midwestern area. These results would provide a closer view of the sources for the ambient aerosols in rural areas of Kentucky and upper Midwestern US and also help develop source emission control strategies to improve the visibility in this area.

2. Sampling and data pretreatment

The Interagency Monitoring of Protected Visual Environments (IMPROVE) monitoring program (Malm et al., 1994; http://vista.cira.colostate.edu/improve) was established in 1985 to support the development of implementation plans for the protection of visibility in 156 national parks and wilderness areas. Particle samples for this study were collected at Mammoth Cave National Park (latitude: 37.13°N; longitude: 86.15°W) during the period from September 1991 to May 2003. Teflon filters were used for mass concentrations and analyzed by Particle Induced X-ray Emission (PIXE) for Na to Mn, by X-ray Fluorescence (XRF) for Fe to Pb and by Proton Elastic Scattering Analysis (PESA) for the elemental hydrogen concentration. Beginning January 1, 2002, XRF was used exclusively for the elemental analysis of Na to Pb. The nylon filter was analyzed via ion chromatography (IC) for nitrate, sulfate and chloride. The quartz filter was analyzed by using IMPROVE/TOR protocol (Chow et al., 1993) for eight temperature-resolved carbon fractions (OC1, OC2, OC3, OC4, OP, EC1, EC2 and EC3; OC: organic carbon; OP: organic pyrolized carbon; EC: elemental carbon). In detail, this protocol volatilizes organic carbon (OC) in four temperature steps in a helium atmosphere: OC1 at 120 °C, OC2 at 250 °C, OC3 at 450 °C, and OC4 at 550 °C. OC4 responses return to constant values. Pyrolyzed organic carbon (OP) is oxidized at 550 °C in a mixture of 2% oxygen and 98% helium atmosphere until the return of filter's reflectance to its initial value. Then, three elemental carbon (EC) fractions are measured in an oxidizing atmosphere: EC1 at 550 °C, EC2 at 700 °C, and EC3 at 850 °C (Begum et al., 2005). In the analyses, OP is reported as a sub-fraction of EC1, but the previous studies (Kim et al., 2004; Kim and Hopke, 2004a,b; Zhao and Hopke, 2004) showed that subtracting OP from EC1 and using OP as an independent species for PMF analysis produced more reasonable results. Thus, OP was separated as a species and EC1 was calculated to be the remaining part of the original measured EC1. After 2000, the IMPROVE program changed the sampling schedule from

24-h samples collected twice per week (on Wednesday and Saturday) to 24-h samples collected every third day.

In the original measurement data set, some species had more than 50% missing or below detection limit (BDL) values. It is not a good method to exclude an element just based on its percentage of missings and BDLs. Recently a practical statistical test based on signal/noise (S/N) ratio was proposed to define the variable (element) quality (Paatero and Hopke, 2003). Elements with the S/N larger than 2 can be considered as good variables, elements with the S/N between 0.2 and 2 can be considered as weak variables, and elements with the S/N less than 0.2 are considered as bad variables. The bad elements should be excluded from analysis. A factor of 2 or 3 can be applied to downweight the weak elements. In addition, the element with more than 90–95% missings and BDLs is recommended to be excluded no matter how much its S/N is. There is a strong relationship between XRF sulfur and IC sulfate, so in accordance with the IMPROVE recommendation (http://vista.cira.colostate.edu/improve), only XRF sulfur was used. Therefore, the PMF analysis began with 1274 samples and 31 species.

3. Data analysis

To identify the number and nature of sources, receptor models are widely used (Hopke, 1985, 1991). For cases without a priori source profile information, principal component analysis (PCA) has been applied (Hopke et al., 1976; Heidam, 1981; Henry, 1987; Barrie and Barrie, 1990). However, Paatero and Tapper (1993) showed that PCA could not provide a true minimal variance solution since it is based on an incorrect weighting scheme. Positive matrix factorization (PMF, Paatero, 1997) is a least squares-based factor analysis model using a data point weighting method and its distinct advantage is the ability to handle missing and below detection limit data by adjusting the corresponding error estimates (Polissar et al., 2001; Song et al., 2001). PMF also implements the non-negativity constraints to obtain more physically realistic factors.

The principle of PMF is briefly presented here. Suppose $\mathbf{X}$ is an n by m data matrix consisting of the measurements of m chemical species in n samples. The objective of multivariate receptor modeling is to determine the number of aerosol sources, p, the chemical composition profiles, $\mathbf{f}_k$, and the contributions, $\mathbf{g}_k$, of sources ($k=1, 2, \ldots, p$) (Polissar et al., 2001; Song et al., 2001). The factor analysis model can be written as

$$\mathbf{X} = \mathbf{G}\mathbf{F}^T + \mathbf{F} \tag{1}$$

where $\mathbf{G}$ is an n by p matrix of source contributions to the samples, $\mathbf{F}^T$ is the transpose of an m by p matrix of source profiles, and $\mathbf{E}$ is a matrix of residuals. Each sample is an observation along the time axis, so $\mathbf{G}$ describes the temporal variation of the source contribution.

The goal of PMF analysis is to determine the number of sources and the corresponding profiles and contributions via solving the optimization problem in Eq. (2).

$$\{\mathbf{G},\mathbf{F}\} = \arg\min_{\mathbf{G},\mathbf{F}}(Q) = \arg\min_{\mathbf{G},\mathbf{F}}\left|\frac{\mathbf{X}-\mathbf{G}\mathbf{F}^T}{\Sigma}\right|^2 \tag{2}$$

where Σ is the uncertainty matrix corresponding to the measurement matrix $\mathbf{X}$. The method for estimating uncertainties was described by Polissar et al. (1998).

4. Results and discussion

Because the sources obtained through PMF are not orthogonal, a solution with more factors does not necessarily contain the same sources in a solution with fewer factors. Therefore, it is necessary to explore different numbers of sources to find the optimal solution with the physical meaning. Generally speaking, finding the solution in PMF can be divided into two steps: coarse selection and fine adjustment.

In the first step, it is expected to determine the proper number of sources through experiments. Q defined in Eq. (2) can be used to help determine the proper source number since it is expected to show a change in slope with the number of sources from rapid to slow at the point of the decided number. More importantly, the resolved sources should be interpretable. In this study, the number of sources was determined to be nine.

In the second step of the analysis, the parameters FPEAK and FKEY are used to control the rotation problem and find the optimal solution, as in general bilinear factor analysis has rotational ambiguity (Paatero et al., 2002). By setting a positive/negative value of FPEAK, the routine is forced to add/subtract **G** factor vectors to/from each other and subtract/add the corresponding **F** factors from/to each other and thereby yields more physically realistic solutions. The details of this procedure are described by Paatero (1997) and Paatero et al. (2002). There is no theoretical rule for selecting FPEAK to produce a "nice" solution. PMF is run with different FPEAK values to determine the range within which the objective function Q does not show a significant change. The optimal solution should lie in this range (Paatero et al., 2002). In this study, Q seemed very stable in the range of FPEAK from -0.2 to 0.2. In view of the physical meaning of the resolved sources and the distribution of the species scaled residuals, the FPEAK value was finally set to 0.

During the step of fine adjustment, chemical compositions of resolved sources may have features that are in disagreement with measured source profiles or prior analyses of similar data. For example, it is not normal for selenium to be presented in significant amount in sea salt rather than in winter coal. Thus, a "pulling down" operation can be used to rotate the system to yield a reasonable profile through the matrix "FKEY" (Lee et al., 1999). This matrix of integer values has the same size as **F**. In general, an FKEY value of 9 corresponds to a "medium–strong" pull.

Additionally, 6 samples were excluded from the final analysis, because they affected the model accuracy and the interpretation of the identified sources. They respectively corresponded to one sharp peak in the initial gasoline contribution series, one sharp peak in the concentration series of K, one sharp peak in the concentration series of EC2, and three sharp peaks in the concentration series of Cu. Such large species peaks relative to the normal range of observed concentrations substantially perturbed the solutions. Since the objective was to apportion the commonly contributing sources, these unusual events were excluded.

Nine sources were resolved for the ambient aerosols at the Mammoth Cave National Park IMPROVE site. They were 1: gasoline emission, 2: diesel emission, 3: summer secondary sulfate, 4: winter secondary sulfate, 5: OP-rich secondary sulfate, 6: secondary nitrate, 7: Intercontinental dust+soil, 8: wood smoke, and 9: aged sea salt. Multiple linear regression (MLR) was applied to regress the total PM$_{2.5}$ mass against the estimated source contributions (Hopke et al., 1980). The regression coefficients should be all positive, if the resolved sources are reasonable. Then, the coefficients were used to scale the source profiles and contributions to make them more physically meaningful. The regression model was also used to reconstruct the PM$_{2.5}$ concentration. Fig. 1 shows the comparison between the reconstructed PM$_{2.5}$ concentration and the measured PM$_{2.5}$ concentration. The slope of the line is 0.85 ± 0.01, the intercept is 1.89 ± 0.15, and R^2 is 0.85,
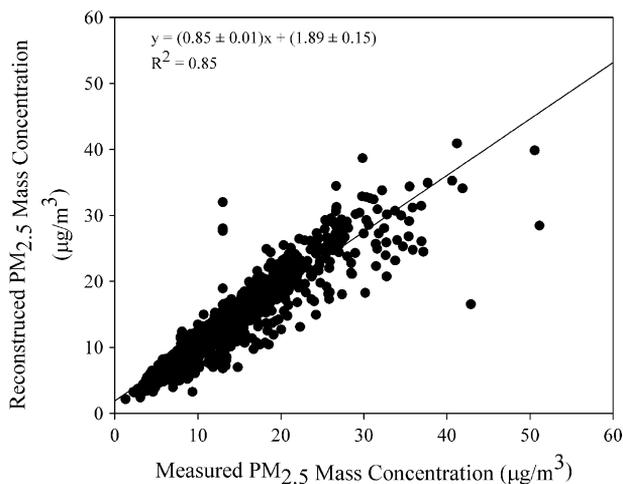
Fig. 1. Comparison of the reconstructed total $PM_{2.5}$ mass concentrations from the PMF analysis with the measured $PM_{2.5}$ mass concentrations.

which means the resolved sources can effectively account for the particle mass. The corresponding source profiles and contributions are shown in Figs. 2 and 3, respectively. The average mass contribution of each source to the total PM mass is shown in Fig. 4.

4.1. Description of diesel and gasoline emissions

Source 1 with high concentrations of OC3 and OC4 and source 2 with high concentration of EC1 represent gasoline and diesel emissions, respectively. Fig. 5 shows the carbon fraction profiles of diesel and gasoline emissions of this study are identical with the profiles of the San Grogonio data, CA (Zhao and Hopke, 2004). Also, they are similar to the profiles estimated in Atlanta, GA (Kim et al., 2004), Washington DC (Kim and Hopke, 2004a), Brigantine, NJ (Kim and Hopke, 2004b), and Bondville, IL (Kim et al., 2005). The diesel emissions contain some Cu, Fe and Zn, because Zn is from the motor oil additives and Cu may be released from brake pads (Garg et al., 2000; Maykut et al., 2003; Kim et al., 2004; Kim and Hopke, 2004a). The Fe is likely to be from muffler ablation. Some Si in the diesel emission profile may be due to the mixture of road dust. The diesel emission profile also shows relatively high concentration of Al. Down-weighting and FPEAK were applied to explore this high value, but there were no significant changes. A possible reason may be that more than 50% of the measurements of Al were missing or below detection limit. The Fe and Ca in the gasoline emission may be mainly from the catalyst-equipped gasoline vehicles (Schauer et al., 2002). Fig. 4 shows that the average contributions of diesel and gasoline emissions to the total PM mass were 3.1% and 6.7%, respectively. The ratio of the diesel emission to the gasoline emission (0.46) is close to that of Brigantine, NJ (Kim and Hopke, 2004b), which indicates possible limited usage of heavy-duty trucks in rural areas. It can be seen from Figs. 6 and 7 that these two sources do not show a significant weekend effect and season (summer/winter) effect. Gasoline emission has a little higher contribution in the weekends, suggesting more gasoline vehicles are used for travel at that time.

Fig. 8 shows a plot of OC3 concentration vs. K concentration that indicates there are two major types of sources in term of OC3 and K. These edges explain why some K is associated
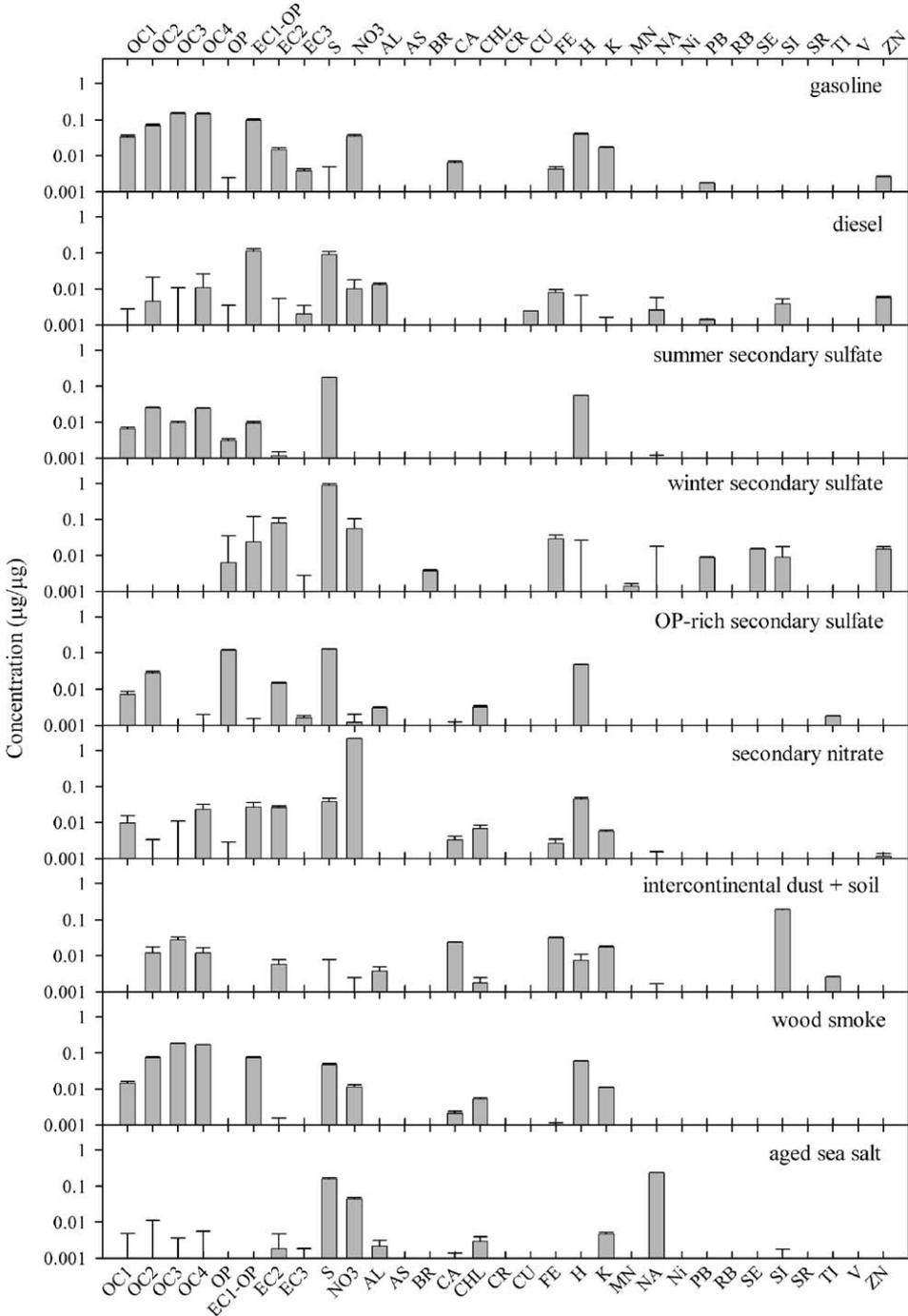
Fig. 2. Profiles of the resolved sources at the Mammoth Cave National Park IMPROVE site.
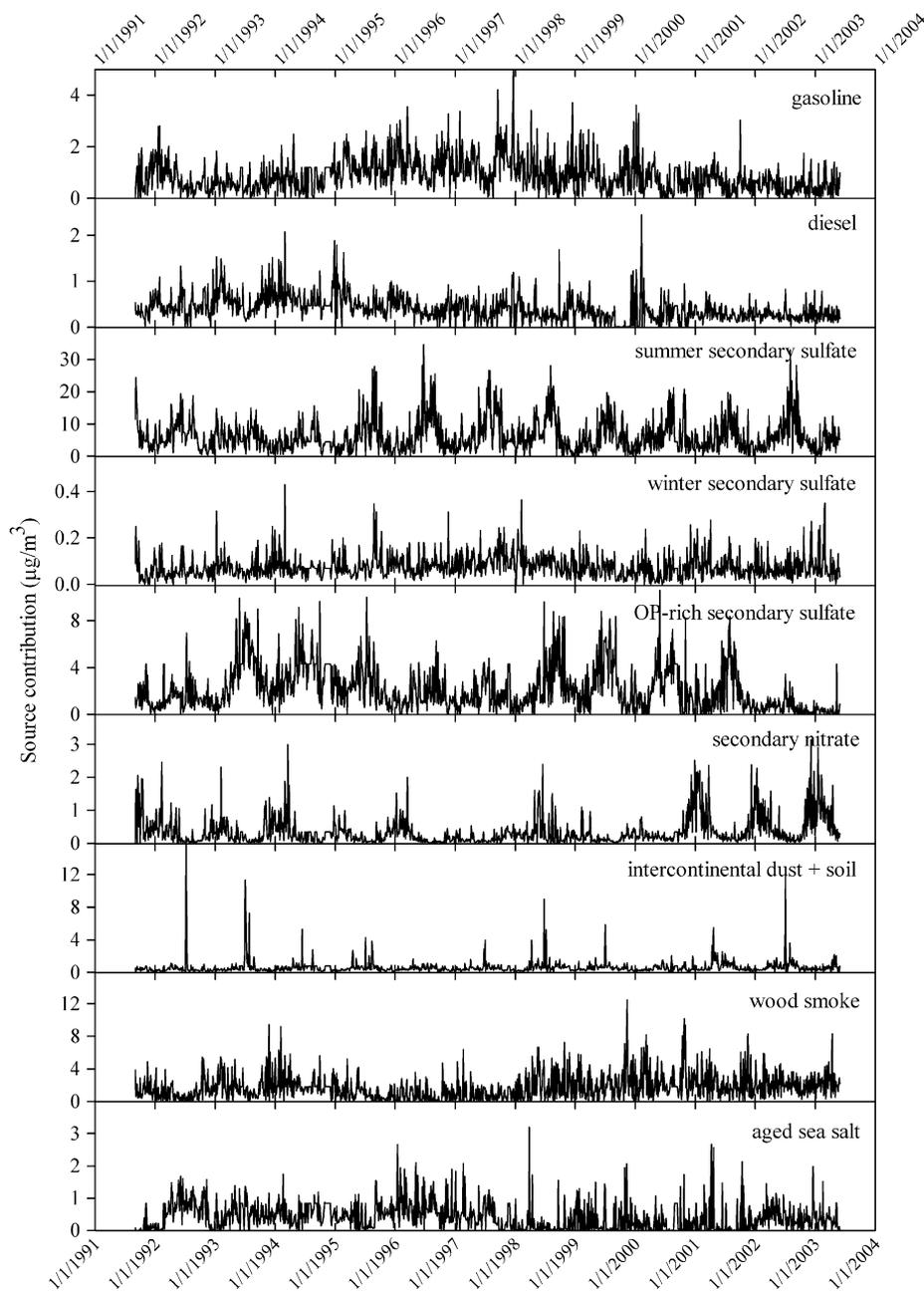
Fig. 3. Contribution time series of the resolved sources at the Mammoth Cave National Park IMPROVE site.

with the gasoline emission source and also some K is associated with source 8 that has been attributed to wood smoke. It is not clear why the K-OC3 relationship is well defined at this site relative to the other IMPROVE data that have been recently studied (Kim and Hopke, 2004a,b; Zhao and Hopke, 2004; Kim et al., 2005).
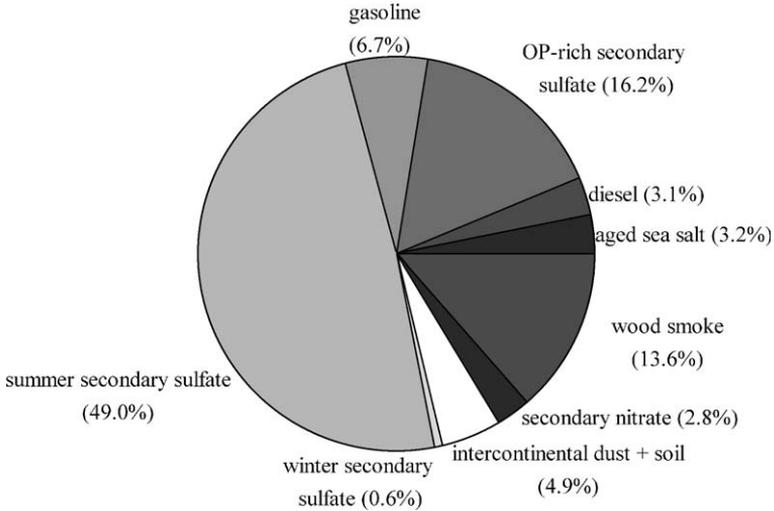
Fig. 4. Relative contributions of the identified sources to the PM$_{2.5}$ mass.

4.2. Description of other sources

In this study, three different secondary sulfate sources with high concentration of S were distinguished. The first secondary sulfate (source 3) represents summer secondary sulfate showing the high contribution peaks in the summer time. Its average contribution to the total PM$_{2.5}$ mass was 49.0%, which was close to the previous study on the Mammoth Cave data (Battelle and Sonoma Technology, Inc., 2002). The relatively high abundance of this source also agrees with the results of a 10-year spatial and temporal trend study of sulfate (Malm et al., 2002). That study found that the SO$_2$ concentrations of the Ohio River Valley and central Tennessee were at least two times those of other regions and that the SO$_4^{2-}$ concentration in southern Kentucky did not show a significant change over the period from 1990 to 1999. The next predominantly sulfur-bearing profile (source 4) shows high concentration of S and some associated Se. Se is the tracer of coal combustion (Polissar et al., 2001) and the contribution
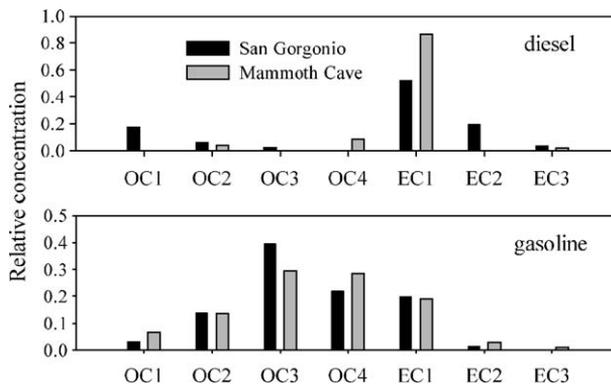

Fig. 5. Comparison of the diesel (top) and gasoline (bottom) carbon thermal fractions extracted from the San Gorgonio site and the Mammoth Cave site.
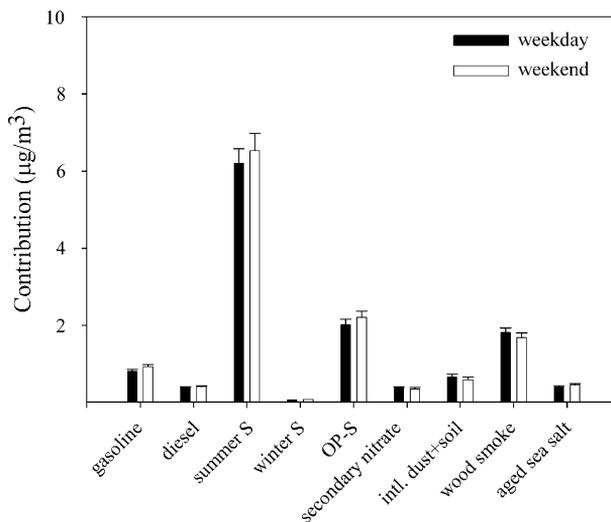
Fig. 6. Comparison of the weekday/weekend contributions for each source at the Mammoth Cave site (mean ± 95% CI).

series shows peaks during the winter months. This source can be called winter secondary sulfate with the contribution to the total $PM_{2.5}$ mass being 0.6%. The third one (source 5) was called OP-rich secondary sulfate with high abundance of OP. This type of factor has been consistently observed in the prior studies that used the IMPROVE thermal fractions (Kim and Hopke, 2004a,b; Kim et al., 2004, 2005). The co-occurrence of OP and S may be due to the additional secondary organic aerosol formation caused by the heterogeneous acidic catalyzed reaction between the acidic SO_4^{2-} and gaseous organic compounds (Jang et al., 2003) and the condensation of semi-volatile organic compounds onto acid sulfate particles. This source contributed 16.2% to the total $PM_{2.5}$ mass.
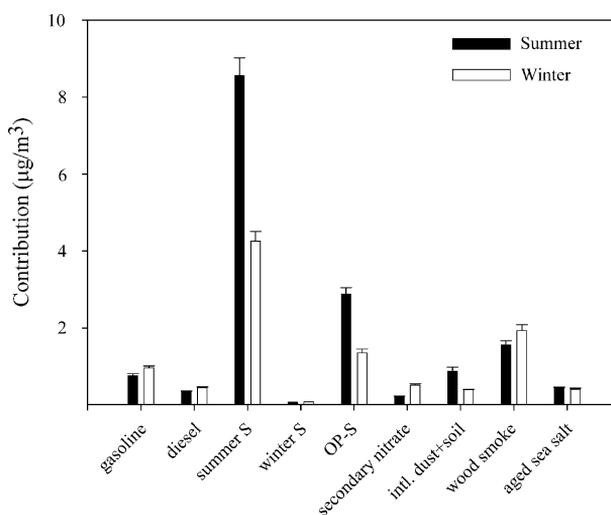

Fig. 7. Comparison of the seasonal (summer: April–September; winter: October–March) contributions for each source at the Mammoth Cave site (mean ± 95% CI).
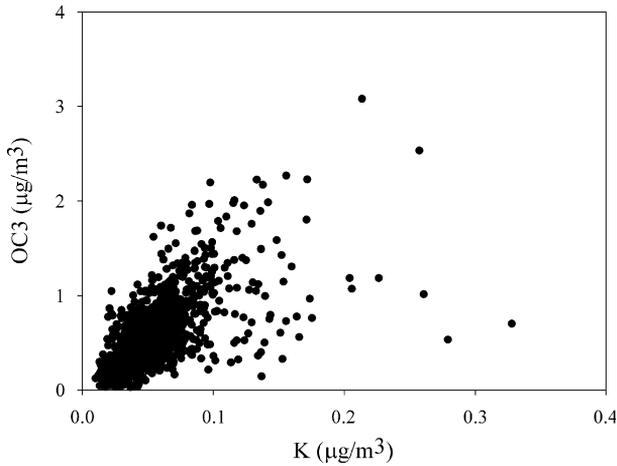
Fig. 8. The concentration of OC3 vs. the concentration of K.

Fig. 9 shows the plot of Se against the S concentrations. The "summer" points are May to September while the "winter" points are October to April. The left edge corresponding to minimum photochemistry shows the higher Se/S ratio while the right edge corresponds to maximal photochemistry with a lower Se/S ratio since the SO_2 emitted with the primary Se is more effectively converted into particulate sulfate. There is less segregation of the winter and summer points relative to other locations like Vermont (Polissar et al., 2001).

Both Figs. 3 and 7 show three different secondary sulfates all have seasonal variations on the contribution series. The Summer secondary sulfate and OP-rich secondary sulfate show summer pattern with the high peaks in the summer time. The high peaks in the summer were due to the higher rate of photo-oxidation reaction at that time, in which SO_2 was changed to SO_4^{2-} (Harrison and Perry, 1986). Due to the high usage of coal in the winter time, the winter secondary sulfate shows winter pattern with the peaks in the winter.

Source 6 is secondary nitrate with high abundance of NO_3^- and contributes 2.8% to the total $PM_{2.5}$ mass. Nitrate is formed in the atmosphere predominantly through oxidation of NO_x and the
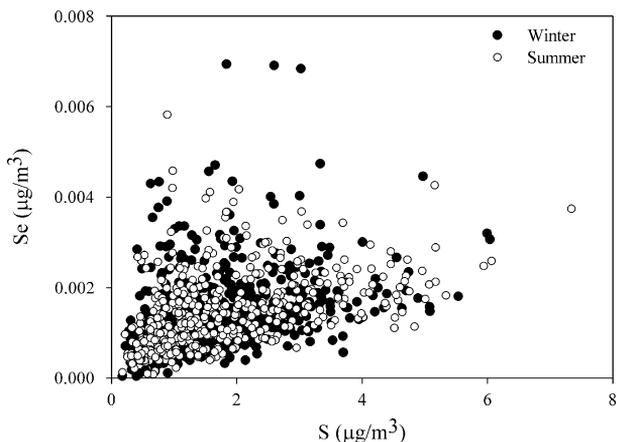

Fig. 9. The concentration of Se vs. the concentration of S.

suspected origin of this material is mobile emissions. This source shows a seasonal trend with high contributions in winter because low temperature shifts the equilibrium system of NO_3^- and HNO_3 toward the particle phase, increasing the mass of NH_4NO_3 (Seinfeld and Pandis, 1998).

Source 7 shows high concentration of Si and its temporal contribution plot shows a number of peaks in the months of June or July. The contribution to these peaks is assigned to Saharan dust (Gatz and Prospero, 1996). In order to assess this hypothesis, air parcel back trajectories on the dates of the high peaks (07/08/1992, 07/03/1993, 06/27/1998, 07/04/2002) were calculated with
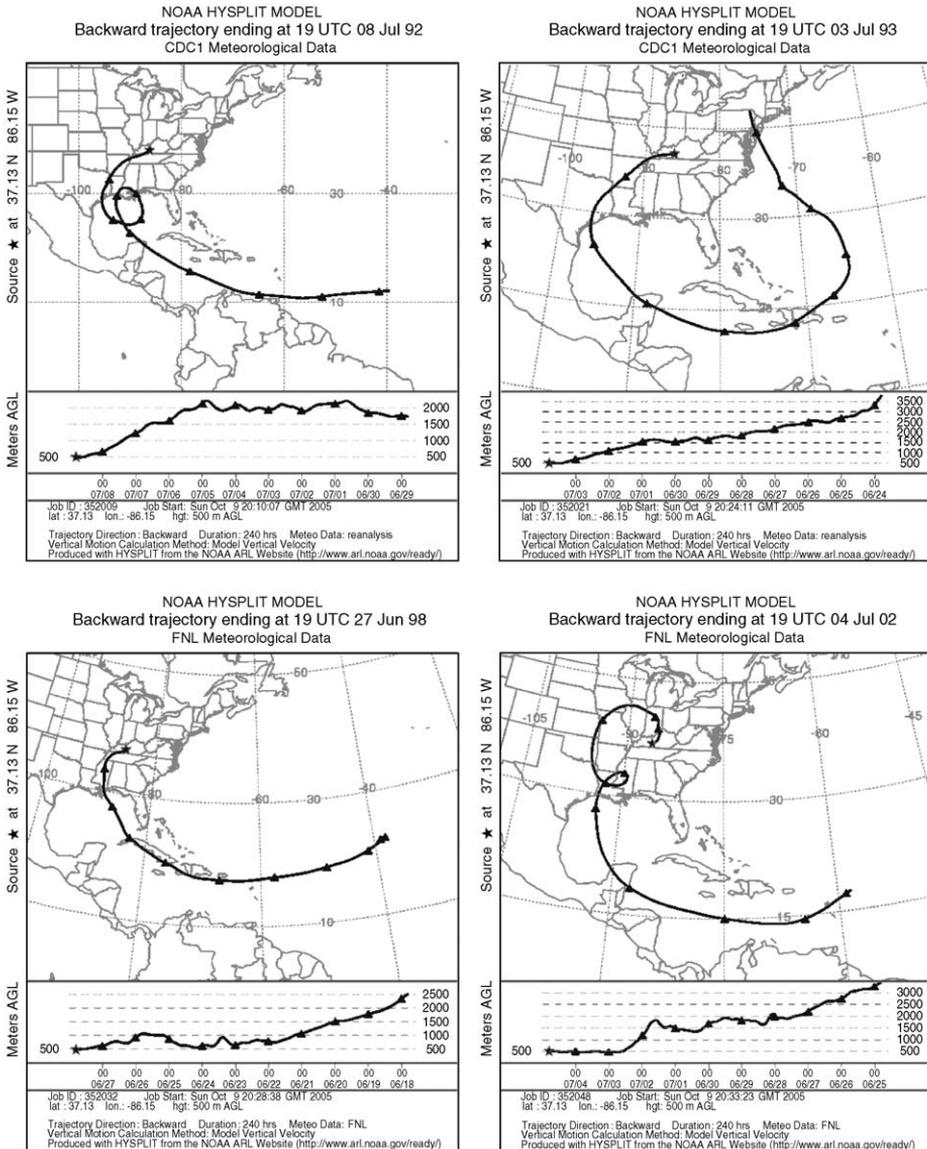

Fig. 10. Calculated backward air parcel trajectory plots for the dates corresponding to four high peaks in the contribution plot of Intercontinental dust + soil.

the NOAA HYSPLIT model (Draxler and Rolph, 2003; Rolph, 2003). The UTC time for back trajectories was selected as 19:00 that corresponded to the noontime at this site. The run time for all the back trajectories was 240 h. Fig. 10 shows three of four back trajectories were through the Atlantic Ocean and the Gulf of Mexico suggesting the dust on these dates were from North Africa. In addition, the study on the Bondville data (Kim et al., 2005) also reported a high peak on 07/04/2002 in the contribution series of airborne soil and the back trajectory for that peak was also through the Atlantic Ocean. The ratio of Si/Ca of the dust from Sahara was around 7 (Gatz and Prospero, 1996). In this study, this ratio was 8.3. The mass percentages of Al and Fe in the Africa dust samples were around 1.67% and 11.30%, respectively (Holmes and Miller, 2004). These two percentages of this study were 1.13% and 9.27%, respectively. These three indexes further support our interpretation of the origin of this source. A small peak on 04/22/2001 was likely to be the Asian sandstorm that developed over Mongolia on 04/07/2001 (NASA, 2001). The study on the Bondville data (Kim et al., 2005) also reported the peak (04/22/2001) in the contribution series of the airborne soil, which provided one more evidence to support the hypothesis of the origin of this factor. This source contributed 4.9% on average to the total $PM_{2.5}$ mass. In Fig. 7, this source shows an obvious summer pattern, suggesting the Saharan dust could be the major contributor to this source.

The profile of source 8 shows high concentration of OCs and some sulfur, H, and K. The temporal contribution of this source shows a seasonal variation with high peaks in winter indicating this source represent wood smoke. The contribution peaks in winter were due to the more usage of wood for warming at that time. This source contributes 13.6% to the total $PM_{2.5}$ mass, which is close to the value previously estimated in the Mammoth Cave data (Battelle and Sonoma Technology, Inc., 2002).

Source 9 represents aged sea salt with high concentrations of Na and S. The low concentration of chloride of this source may be due to the conversion from NaCl to Na_2SO_4 by interaction with gas phase SO_2 or through cloud processing. This source contributes 3.2% to the total $PM_{2.5}$ mass. This source does not show significant seasonal and weekend effects.

5. Conclusion

The chemical composition data of the ambient aerosols collected at the Mammoth Cave National Park IMPROVE site were studied using PMF to identify the possible emission sources for the aerosols in the rural upper-Midwestern areas. The results of this study can be summarized as: 1) the feasibility of applying PMF to separate gasoline/diesel emissions in the rural Midwestern area with carbon fractions was further demonstrated; 2) the other seven sources, aged sea salt, summer secondary sulfate, winter secondary sulfate, OP-rich secondary sulfate, secondary nitrate, and wood smoke, and Saharan red sand dust, were identified; 3) summer secondary sulfate, OP-rich secondary sulfate, and wood smoke were three major sources for the ambient aerosols at the Mammoth Cave National Park site; and 4) the contributions of Saharan sandstorm were observed.

References

Barrie, L.A., Barrie, M.J., 1990. Chemical components of lower tropospheric aerosols in the high Arctic: six years of observations. Atmos. Chem. 11, 211–226.

Battelle and Sonoma Technology, Inc., 2002. http://www.marama.org/visibility/SA_report/.

Begum, B.A., Hopke, P.K., Zhao, W., 2005. Source identification of fine particles in Washington, DC, by expanded factor analysis modeling. Environ. Sci. Technol. 39, 1129–1137.

Brauer, M., Hoek, G., van Vliet, P., Meliefste, K., Fischer, P.H., Wijga, A., Koopman, L.P., Neijens, H.J., Gerritsen, J., Kerkhof, M., Heinrich, J., Bellander, T., Brunekreef, B., 2002. Air pollution from traffic and the development of respiratory infections and asthmatic and allergic symptoms in children. Am. J. Respiratory Crit. Care Med. 166, 1092–1098.

Brauer, M., Hoek, G., Van Vliet, P., Meliefste, K., Fischer, P., Gehring, U., Heinrich, J., Cyrys, J., Bellander, T., Lewne, M., Brunekreef, B., 2003. Estimating long-term average particulate air pollution concentrations: application of traffic indicators and geographic information systems. Epidemiology 14, 228–239.

Chow, J.W., Waston, J.G., Pritchett, L.C., Pierson, W.R., Fraizer, C.A., Purcell, R.G., 1993. The DRI thermal/optical reflectance carbon analysis system: description, evaluation and applications in U.S. air quality studies. Atmos. Environ. 27A, 1185–1201.

Cyrys, J., Heinrich, J., Hoek, G., Meliefste, K., Lewne, M., Gehring, U., Bellander, T., Fischer, P., Van Vliet, P., Brauer, M., Wichmann, H.E., Brunekreef, B., 2003. Comparison between different traffic-related particle indicators: elemental. carbon (EC), $PM_{2.5}$ mass, and absorbance. J. Expo. Anal. Environ. Epidemiol. 13, 134–143.

de Hartog, J.J., Hoek, G., Peters, A., Timonen, K.L., Ibald-Mulli, A., Brunekreef, B., Heinrich, J., Tiittanen, P., van Wijnen, J.H., Kreyling, W., Kulmala, M., Pekkanen, J., 2003. Effects of fine and ultrafine particles on cardiorespiratory symptoms in elderly subjects with coronary heart disease — The ULTRA study. Am. J. Epidemiol. 157, 613–623.

Draxler, R.R., Rolph, G.D., 2003. HYSPLIT (HYbrid Single-Particle Lagrangian Integrated Trajectory) Model access via NOAA ARL READY Website (http://www.arl.noaa.gov/ready/hysplit4.html). NOAA Air Resources Laboratory, Silver Spring, MD.

Dockery, D.W., Pope, C.A., Xu, X.P., Spengler, J.D., Ware, J.H., Fay, M.E., Ferris, B., Speizer, F.E., 1993. An association between air-pollution and mortality in 6 United-States cities. N. Engl. J. Med. 329, 1753–1759.

Gauderman, W.J., McConnell, R., Gilliland, F., London, S., Thomas, D., Avol, E., Vora, H., Berhane, K., Rappaport, E.B., Lurmann, F., Margolis, H.G., Peters, J., 2000. Association between air pollution and lung function growth in southern California children. Am. J. Respir. Crit. Care Med. 162, 1383–1390.

Garg, B.D., Cadle, S.H., Mulawa, P.A., Groblicki, P.J., Laroo, C., Parr, G.A., 2000. Brake wear particulate matter emissions. Environ. Sci. Technol. 34, 4463–4469.

Gatz, D.F., Prospero, J.M., 1996. A large silicon–aluminum aerosol plume in central Illinois: North Africa desert dust? Atmos. Environ. 30, 3789–3799.

Harrison, R.M., Perry, R., 1986. Handbook of Air Pollution Analysis, Second edition. Chapman and Hall.

Heidam, N.Z., 1981. On the origin of the arctic aerosol — a statistical approach. Atmos. Environ. 15, 1421–1427.

Henry, R.C., 1987. Current factor analysis receptor models are ill-posed. Atmos. Environ. 21, 1815–1820.

Hoek, G., Brunekreef, B., Goldbohm, S., Fischer, P., van den Brandt, P.A., 2002. Association between mortality and indicators of traffic-related air pollution in The Netherlands: a cohort study. Lancet 360, 1203–1209.

Holmes, C.W., Miller, R., 2004. Atmospherically transported elements and deposition in the southeastern United States: local or transoceanic? Appl. Geochem. (19), 1189–1200.

Hopke, P.K., 1985. Receptor Modeling in Environmental Chemistry. J. Wiley & Sons, Inc., New York.

Hopke, P.K., 1991. Receptor Modeling for Air Quality Management. Elsevier, Amsterdam.

Hopke, P.K., Gladney, E.S., Gordon, G.E., Zoller, W.H., Jones, A.G., 1976. The use of multivariate analysis to identify sources of selected elements in the Boston urban aerosol. Atmos. Environ. 10, 1015–1025.

Hopke, P.K., Lamb, R.E., Natusch, D., 1980. Multielemental characterization of urban roadway dust. Environ. Sci. Technol. 14, 164–172.

Jang, M., Lee, S., Kamens, R.M., 2003. Organic aerosol growth by acid-catalyzed heterogeneous reactions of octanal in a flow reactor. Atmos. Environ. 37, 2125–2138.

Kim, E., Hopke, P.K., 2004a. Source apportionment of fine particles at Washington, DC utilizing temperature resolved carbon fractions. J. Air Waste Manage. Assoc. 54, 773–785.

Kim, E., Hopke, P.K., 2004b. Improving source identification of fine particles in a rural northeastern U.S. area utilizing temperature resolved carbon fractions. J. Geophys. Res. 109 (109), D09204.

Kim, E., Hopke, P.K., Edgerton, E.S., 2004. Improving source identification of Atlanta aerosol using temperature resolved carbon fractions in positive matrix factorization. Atmos. Environ. 38, 3349–3362.

Kim, E., Hopke, P.K., Kenski, D.M., Koerber, M., 2005. Sources of in a rural Midwestern U.S. area. Environ. Sci. Technol. 39, 4953–4960.

Lee, E., Chan, C.K., Paatero, P., 1999. Application of positive matrix factorization in source apportionment of particulate pollutants in Hong Kong. Atmos. Environ. 33, 3201–3212.

Malm, W.C., Sisler, J.F., Huffman, D., Eldred, R.A., Cahill, T.A., 1994. Spatial and seasonal trends in particle concentration and optical extinction in the United States. J. Geophys. Res. 99, 1347–1370.

Malm, W.C., Schichtel, B.A., Ames, R.B., Gebhart, K.A., 2002. A 10-year spatial and temporal trend of sulfate across the United States. J. Geophys. Res. 107 (D22).

Maykut, N.N., Lewtas, J., Kim, E., Larson, T.V., 2003. Source apportionment of $PM_{2.5}$ at an urban IMPROVE site in Seattle, Washington. Environ. Sci. Technol. 37, 5135–5142.

NASA, 2001. Earth probe total ozone mapping spectrometer aerosol index, http://toms.gsfc.nasa.gov/aerosols/aerosols.html.

Paatero, P., 1997. Least squares formulation of robust, non-negative factor analysis. Chemom. Intell. Lab. Syst., Lab. Inf. Manag. 37, 23–35.

Paatero, P., Hopke, P.K., 2003. Discarding or downweighting high noise variables in factor analytic models. Anal. Chim. Acta 490, 277–289.

Paatero, P., Tapper, U., 1993. Analysis of different modes of factor analysis at least squares fit problems. Chemom. Intell. Lab. Syst., Lab. Inf. Manag. 18, 183–194.

Paatero, P., Hopke, P.K., Song, X.-H., Ramadan, Z., 2002. Understanding and controlling rotations in factor analytic models. Chemom. Intell. Lab. Syst., Lab. Inf. Manag. 60, 253–264.

Polissar, A.V., Hopke, P.K., Malm, W.C., Sisler, J.F., 1998. Atmospheric aerosol over Alaska: 2. Elemental composition and sources. J. Geophys. Res. 103, 19045–19057.

Polissar, A.V., Hopke, P.K., Poirot, R.L., 2001. Atmospheric aerosol over Vermont chemical composition and sources. Environ. Sci. Technol. 35, 4604–4621.

Rolph, G.D., 2003. Real-time Environmental Applications and Display sYstem (READY) Website (http://www.arl.noaa.gov/ready/hysplit4.html). NOAA Air Resources Laboratory, Silver Spring, MD.

Schauer, J.J., Kleeman, M.J., Cass, G.R., Simoneit, B.R.T., 2002. Measurement of emissions from air pollution sources: 5. C_1–C_{32} organic compounds from gasoline-powered motor vehicles. Environ. Sci. Technol. 36, 1169–1180.

Seinfeld, J.H., Pandis, S.N., 1998. Atmospheric Chemistry and Physics: From Air Pollution to Climate Change. John Wiley and Sons, Inc..

Song, X., Polissar, A.V., Hopke, P.K., 2001. Sources of fine particle composition in the northeastern US. Atmos. Environ. 35, 5277–5286.

Zhao, W., Hopke, P.K., 2004. Source apportionment of ambient particles in the San Gorgonio Wildness. Atmos. Environ. 38, 5901–5910.